# Data-mining-assisted resonance labeling in ring-based DWDM transceivers

**Peng Sun, Jared Hulme, Ashkan Seyedi, Marco Fiorentino, Raymond Beausoleil**
*Hewlett Packard Laboratories, 1501 Page Mill Rd., Palo Alto, CA 94304*
*psun@hpe.com*

**Abstract:** An algorithm using hierarchical clustering is proposed to label resonances in ring-based DWDM transceivers. By identifying missing resonances and split-peaks due to reflection, the algorithm enables binning of individual ring resonances by passive optical tests.
**OCIS codes:** 060.4230, 130.6750, 230.5750.

## 1. Introduction

Ring-based Dense Wavelength-Division-Multiplexing (DWDM) transceivers have the potential to achieve high bandwidth density and low power consumption within small footprints [1]. It is challenging to sort and bin each and every ring channel at the wafer scale with passive optical tests, as the transmission spectra of multi-ring transceivers are distorted by a multitude of factors. First, reflection in the ring waveguides may cause the resonances to have split-peaks instead of a single Lorentzian line shape [2]. Second, intra-reticle process variation causes the resonances to partially or completely overlap with neighboring resonances. Not helping the issue is that the resonance detection algorithm cannot always detect all resonances correctly, nor distinguish split-peaks of one ring from two peaks of two neighboring rings. To resolve the ambiguity, phase modulation using thermo-optic effect or plasma dispersion effect can be applied to shift an individual ring's resonances while leaving those of the other rings unaffected. This procedure requires multiple electrical probing together with optical probing, which add significant time and complexity to the wafer sorting. It is highly desirable to resolve ambiguity and label the resonances with passive optical tests only. In this paper, we devised an algorithm to detect and label resonances in multi-ring DWDM transmitters (Tx) and receivers (Rx), including missing resonances and split-peaks. This capability enables sorting and binning individual rings with passive optical tests without resorting to electrical phase shifters.

## 2. Design, Fabrication, and Testing

One Tx loop and one Rx loop are laid out within the full reticle. For each Tx/Rx loop, 24 ring resonators are coupled to the same bus waveguide, which is terminated with two identical grating couplers that couple light between an array of two polarization-maintaining single-mode fibers and the input/through ports of the loop. The drop ports of all rings are terminated with Ge photodetectors (PD), and the add ports are all terminated with waveguide terminations. Rings in the Tx loop are critically coupled with through and drop gap widths of 175nm and 200nm respectively; rings in the Rx are slightly under coupled with through and drop gaps of 200nm and 200nm respectively. The bus waveguides are 330nm in width, and the ring waveguides are 450nm in width. A schematic drawing of the Tx/Rx test loop is shown in Fig.1a. The rings' radii increase linearly from 5um of the first ring to 5.046um of the last ring at a step size of 2nm. The channel-to-channel spacing is about 0.35nm, and the free-spectral range (FSR) is about 13.3nm.

The Tx/Rx loops were taped out at STMicroelectronics using the DAPHNE technology on 300mm SOI wafers, which have 300nm silicon layer on top of 720nm buried oxide layer. The top silicon layer is patterned with conventional 193nm lithography in 55nm CMOS node. The ring resonators are formed by etching 250nm into the silicon layer, and the grating couplers are formed by etching 140nm into the silicon layer. The ring resonators are doped to form PIN junctions for optical modulation by carrier injection. P-type resistive heaters are also formed within the rings to tune the resonances by thermo-optic effect. Layout of one ring resonator with the PIN junction doping as well as the resistive heater is shown in Fig.1b.

A tunable laser is coupled to the input port, and the output light is collected by a photodetector. The laser wavelength is scanned from 1280nm to 1360nm at a step size of 2pm, and the laser output power is set to 0dBm, which does not cause significant nonlinear effects in the ring resonators. This work contains only passive optical tests; the resistive heaters and the PIN diodes are not used. All 66 testable full dies on one 300mm full-flow wafer are tested. A typical transmission spectrum is shown in Fig.1c, which is tested on the Tx loop on die 5. The transmission spectrum consists of 6 resonance bands, each of which contains about 24 individual resonances due to the 24 rings. In Fig.1c the parabolic fitted envelop of the grating couplers' spectral response is also shown in red, which will be used to normalize the transmission spectrum in the following analysis.

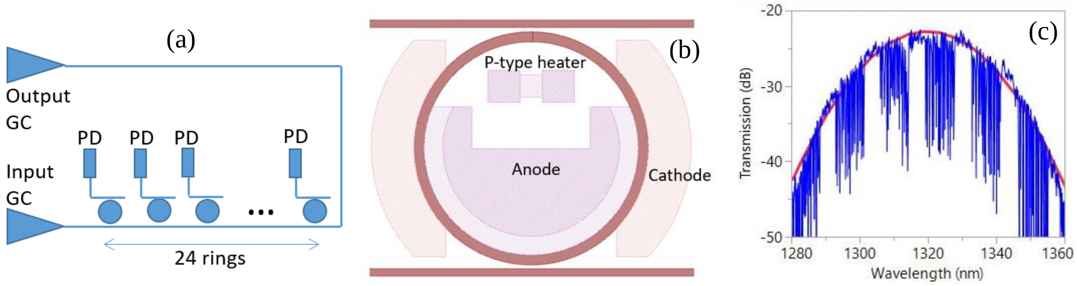


Fig. 1. (a) Schematic of the 24-ring Tx/Rx test loop. (b) Layout of one ring resonator. (c) Tested transmission spectrum of the Tx loop (blue) and parabolic fitted envelop (red) on die 5.

## 3. Data Analysis

The transmission spectra of the tested Tx/Rx loops are normalized with respect to the envelope and converted to linear scale. Continuous-Wavelet Transform (CWT) is then performed on the spectra to detect resonances [3]. In this paper, we choose Ricker's wavelet with width from 36pm to 120pm for 200 steps, and minimal signal to noise ratio of 1.0. Resonances of both Tx and Rx loops on all 66 tested dies of the wafer are shown in Fig.2a, where the 6 resonance bands across the laser sweep range are color coded. Fig.2b shows part of the Rx spectrum on die 5, where 29 resonances within the band 3 (~1310nm) are detected as the CWT algorithm cannot determine whether the closely spaced twin resonances are split-peaks of a single resonance, or two resonances of two neighboring rings. The numbers of resonances detected in each band for all bands on all dies of the wafer are shown in Fig.2c. It can be seen that majority of the bands have more resonances than the expected 24 resonances due to split-peaks, and a few bands have fewer resonances than 24 due to missing resonances.

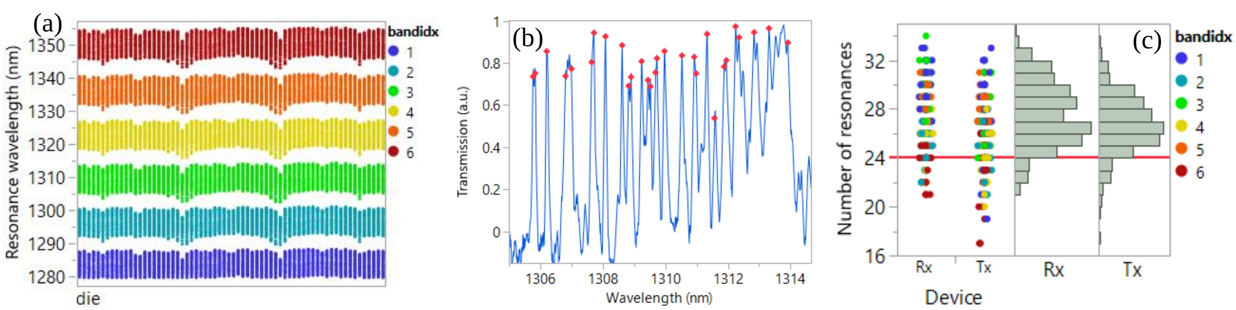


Fig. 2. (a) Resonances of both Tx and Rx loops on all 66 dies of the tested wafer. (b) Normalized and inverted transmission spectrum of the Rx on die 5. Raw data is shown in blue and CWT-detected resonances in red. (c) Number of resonances detected in each band for all 6 bands on all dies.

In this paper we devised a method to better detect and label resonances in the multi-ring Tx/Rx loops. One important piece of information that was not utilized in the CWT-based peak detection is the periodic repetition of a ring's resonances, which lie on an approximately linear wavelength grid. By shifting and overlaying resonances across all bands, the problem of peak detection and labeling is converted to hierarchical clustering that groups the resonance wavelengths into an expected number of clusters, which in this analysis is set to the number of rings per Tx/Rx. There are three reasons that the resonance detection and labeling can be improved by taking into account all the resonance bands within the laser scan range. First, reflection induced by the ring's waveguide sidewall roughness varies with wavelength and creates different resonance splitting characteristics across different bands of the same ring. In other words, split-peaks of one ring in one band are unlikely to remain split-peaks of the same spacing across all bands, while the spacing between two resonances of two neighboring rings will remain largely constant across all bands barring the ~1% band-to-band shrinking in spacing due to dispersion and mode order change. By overlaying and comparing resonances of different bands, split-peaks of one resonance can be differentiated from two resonances of two rings. It is worth noting that such inference is probabilistic instead of deterministic. Second, the CWT peak detection algorithm may occasionally fail to detect one resonance within one band due to noise or spectral distortion, but the possibility that multiple resonances of the same ring are missed out across multiple bands diminishes as the number of bands increases. Hence it is possible to label missing resonances by comparing resonances in different bands based on probability. Third, we choose Ward's linkage criterion in the hierarchical cluster analysis, which minimizes the within-cluster variance. More resonance bands and larger number of resonances in each cluster will yield more accurate estimation of variance and more robust clustering.

The proposed algorithm is exemplified in the following. Fig.3a shows transmission spectra of the 6 bands of the Rx loop on die 5, where each band is shifted as a whole to minimize the sum of distances of all resonances within the band to their respective nearest neighbors in the previous band. Channel-to-channel spacing increases approximately linearly by ~0.7% between two neighboring bands, which causes a keystone effect in Fig.3a. The keystone effect is due to both the dispersion of ring waveguide's effective index and the different resonance orders of different bands. Calculations predict ~1% increase in channel spacing between neighboring bands, which agrees reasonably well with the test results. The keystone effect is corrected for by linearly stretching lower bands and compressing higher bands. Fig.3b shows the results of the hierarchical clustering using Ward's linkage criterion and the number of clusters equal to 24, where the resonances are color coded and marked by the cluster number. It can be seen that split-peaks such as channel 1 band 3 (red circle) can be distinguished from two resonances of neighboring rings such as channels 3 and 4 (blue diamond and brown cross); missing resonances such as channel 5 band 4 (cyan triangle) are also identified. Fig.3c shows an example bin map of the 1310nm band of the tested wafer: within each of the 66 tested dies, the bin is plotted versus the 24 channels. The bins are defined as following: missing resonances in either Tx or Rx are labeled as bin 9; Tx-Rx channel pairs that have larger offsets than 3σ of the distribution of the Tx-Rx channel offset are labeled as bin 6; split-peaks in Tx or Rx as bin 1; others as bin 0. Devices in bins 0/1 can in general be considered acceptable, while devices in bins 6 and 9 need to be tested further at wafer or die scale. Knowledge of the channel position of the missing resonances in the resonance banks helps expedite the follow-up tests that may involve both electrical and optical probing.

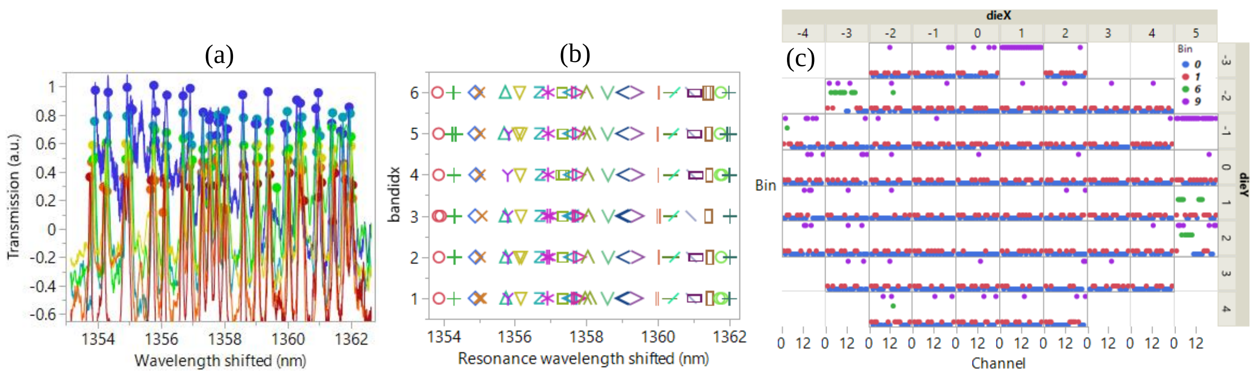


Fig. 3. a) Transmission spectrum of the Rx loop on die 5 shifted and overlaid. b) Hierarchical clustering results of the Rx resonances on die 5. (c) Example wafer bin map for all 24 channels in the 1310nm band.

## 4. Conclusions

By shifting and overlaying resonances of multiple bands, hierarchical clustering enables robust and comprehensive labeling of resonances in ring-based DWDM Tx/Rx loops with passive optical tests only. Split-peaks due to reflection of one ring can be distinguished from two peaks of two resonances, and missing resonances can also be labeled. This capability simplifies the optical sorting procedures and saves testing time.

## References

[1] M. A. Seyedi, J. Hulme, P. Sun, T. Van Vaerenbergh, X. Zeng, G. Kurczveil, Z. Huang, D. Liang, M. Fiorentino, Ray Beausoleil, "Overview of silicon photonics components for commercial DWDM applications," OSA Advanced Photonics Congress 2019, paper ITh1A.3.

[2] A. Li, T. Van Vaerenbergh, P. Heyn, P. Bienstman, W. Bogaerts, "Backscattering in silicon microring resonators: a quantitative analysis," Laser & Photon. Rev. 10:420-431, (2016).

[3] P. Du, W.A. Kibbe, S.M. Lin, "Improved peak detection in mass spectrum by incorporating continuous wavelet transform-based pattern matching," Bioinformatics, vol. 22, issue 17, pp.2059-2065, (2006).